Elastic Wave Propagation in Circumferential Direction in Anisotropic Cylindrical Curved Plates

S. Towfighi

T. Kundu
Fellow ASME

M. Ehsani
Department of Civil Engineering
and Engineering Mechanics,
University of Arizona,
Tucson, AZ 85721

Ultrasonic nondestructive inspection of large-diameter pipes is important for health monitoring of ailing infrastructure. Longitudinal stress-corrosion cracks are detected more efficiently by inducing circumferential waves; hence, the study of elastic wave propagation in the circumferential direction in a pipe wall is essential. The current state of knowledge lacks a complete solution of this problem. Only when the pipe material is isotropic a solution of the wave propagation problem in the circumferential direction exists. Ultrasonic inspections of reinforced concrete pipes and pipes retrofitted by fiber composites necessitate the development of a new theoretical solution for elastic wave propagation in anisotropic curved plates in the circumferential direction. Mathematical modeling of the problem to obtain dispersion curves for curved anisotropic plates leads to coupled differential equations. Unlike isotropic materials for which the Stokes-Helmholtz decomposition technique simplifies the problem, in anisotropic case no such general decomposition technique works. These coupled differential equations are solved in this paper. Dispersion curves for anisotropic curved plates of different curvatures have been computed and presented. Some numerical results computed by the new technique have been compared with those available in the literature. [DOI: 10.1115/1.1464872]

Introduction

Mathematical modeling of wave propagation in the axial direction of a cylinder has been studied extensively. However, for wave propagation in the circumferential direction, which is essential for nondestructive testing (NDT) of large diameter pipes, literature shows fewer investigations. Viktorov's work ([1]) establishes the fundamental mathematical modeling of the problem for isotropic material properties. He has introduced the angular wave number concept and has derived, decomposed and solved the governing differential equations. He has considered only one curved surface; in other words, he has found the solution for convex and concave cylindrical surfaces. In order to obtain the results for curved plates Qu et al. [2] have added the boundary conditions for the second surface and solved the problem of guided wave propagation in isotropic curved plates. Different aspects of the circumferential direction wave propagation along one or multiple curved surfaces have been analyzed by Grace and Goodman [3], Brekhovskikh [4], Cerv [5], Liu and Qu [6,7] and Valle, Qu, and Jacobs [8]. In all these works the material has been modeled as isotropic elastic material.

Many investigators have solved elastic wave propagation problem in homogeneous and multilayered anisotropic solids. However, all those works have been limited to the flat-plate case ([9]) or for waves propagating in the axial direction of a cylinder ([10]). Wave propagation in the circumferential direction of an anisotropic curved plate has not been analyzed earlier, and solved for the first time in this paper.

Unlike isotropic materials for which the Stokes-Helmholtz decomposition technique simplifies the problem, for anisotropic case no such general decomposition technique works. The differential equations remain coupled and require a more general solution technique.

The new technique, presented in this paper, solves coupled set of differential equations without attempting to decouple the equations. Hence it removes the obstacle arising from not being able to decouple the equations. Consequently it provides a systematic and unifying solution method, which is capable of solving a set of coupled differential equations, and can be utilized to solve a variety of wave propagation problems.

Fundamental Equations

The formulation presented here is for the wave propagation in a cylindrical curved plate in the direction of the curvature as shown in Fig. 1. We will interchangeably call the wave carrier a ''curved plate,'' ''cylinder,'' ''pipe segment,'' or simply ''pipe'' all meaning the same thing. What we are interested in is analyzing the dispersive waves in the curved plate for waves propagating from section T to R (see Fig. 1). This analysis does not include the reflected guided waves from the plate boundary. The problem geometry can be a segment of a cylinder or a complete cylinder.

Wave propagation in circumferential direction in pipes with isotropic material properties is usually modeled as a plane strain problem; i.e., the displacement component along the longitudinal axis of the pipe is set equal to zero. For a few other types of anisotropy this situation remains valid. However, for general anisotropy the longitudinal component of displacement must be considered in the mathematical modeling. The symmetry of both geometry and material properties is required for plane-strain idealization. In absence of such symmetry a three-dimensional mathematical modeling is necessary.

In cylindrical coordinates, strain components in terms of displacements can be written as

Contributed by the Applied Mechanics Division of THE AMERICAN SOCIETY OF MECHANICAL ENGINEERS for publication in the ASME JOURNAL OF APPLIED MECHANICS. Manuscript received by the ASME Applied Mechanics Division, April 5, 2001; final revision, November 1, 2001. Associate Editor: A. K. Mal. Discussion on the paper should be addressed to the Editor, Prof. Lewis T. Wheeler, Department of Mechanical Engineering, University of Houston, Houston, TX 77204-4792, and will be accepted until four months after final publication of the paper itself in the ASME JOURNAL OF APPLIED MECHANICS.

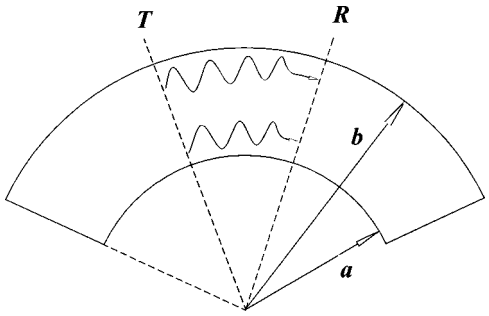

Fig. 1 Waves propagating from section *T* to *R* in a curved plate. Wave speed is proportional to radius of curvature.

$$e_{rr}=\frac{\partial u_r(r,\theta,t)}{\partial r}$$

$$e_{\theta\theta}=\frac{\partial u_\theta(r,\theta,t)}{r\partial\theta}+\frac{1}{r}u_r(r,\theta,t)$$

$$e_{zz}=\frac{\partial u_z(r,\theta,t)}{\partial z}$$

$$e_{r\theta}=\frac{1}{2}\left(\frac{\partial u_r(r,\theta,t)}{r\partial\theta}+\frac{\partial u_\theta(r,\theta,t)}{\partial r}-\frac{u_\theta(r,\theta,t)}{r}\right)$$

$$e_{\theta z}=\frac{1}{2}\left(\frac{\partial u_z(r,\theta,t)}{r\partial\theta}+\frac{\partial u_\theta(r,\theta,t)}{\partial z}\right)$$

$$e_{rz}=\frac{1}{2}\left(\frac{\partial u_r(r,\theta,t)}{\partial z}+\frac{\partial u_z(r,\theta,t)}{\partial r}\right). \tag{1}$$

The stress and displacement components are shown in Fig. 2. And constitutive matrix for general anisotropy contains 21 independent elastic constants:

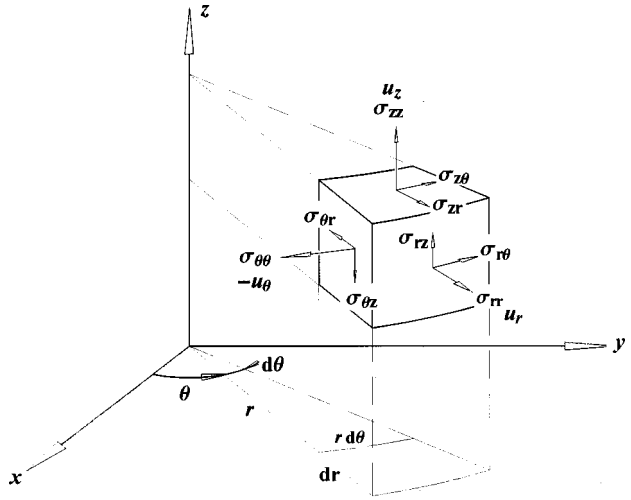

Fig. 2 Stress and displacement components in cylindrical coordinate system

$$\begin{pmatrix}\sigma_{\theta,\theta}\\ \sigma_{z,z}\\ \sigma_{r,r}\\ \sigma_{\theta,z}\\ \sigma_{r,\theta}\\ \sigma_{r,z}\end{pmatrix}=\begin{pmatrix}C_{1,1}&C_{1,2}&C_{1,3}&C_{1,4}&C_{1,5}&C_{1,6}\\ C_{1,2}&C_{2,2}&C_{2,3}&C_{2,4}&C_{2,5}&C_{2,6}\\ C_{1,3}&C_{2,3}&C_{3,3}&C_{3,4}&C_{3,5}&C_{3,6}\\ C_{1,4}&C_{2,4}&C_{3,4}&C_{4,4}&C_{4,5}&C_{4,6}\\ C_{1,5}&C_{2,5}&C_{3,5}&C_{4,5}&C_{5,5}&C_{5,6}\\ C_{1,6}&C_{2,6}&C_{3,6}&C_{4,6}&C_{5,6}&C_{6,6}\end{pmatrix}\cdot\begin{pmatrix}e_{\theta,\theta}\\ e_{z,z}\\ e_{r,r}\\ 2e_{\theta,z}\\ 2e_{r,\theta}\\ 2e_{r,z}\end{pmatrix}. \tag{2}$$

Equations of motion for three components of displacement in cylindrical coordinates are as follows:

$$\frac{\partial\sigma_{rr}}{\partial r}+\frac{\partial\sigma_{rz}}{\partial z}+\frac{\partial\sigma_{r\theta}}{r\partial\theta}+\frac{\sigma_{rr}-\sigma_{\theta\theta}}{r}-\rho\frac{\partial^2u_r(r,\theta,t)}{\partial t^2}=0$$

$$\frac{\partial\sigma_{r\theta}}{\partial r}+\frac{\partial\sigma_{\theta z}}{\partial z}+\frac{\partial\sigma_{\theta\theta}}{r\partial\theta}+\frac{2\sigma_{r\theta}}{r}-\rho\frac{\partial^2u_\theta(r,\theta,t)}{\partial t^2}=0$$

$$\frac{\partial\sigma_{rz}}{\partial r}+\frac{\partial\sigma_{zz}}{\partial z}+\frac{\partial\sigma_{\theta z}}{r\partial\theta}+\frac{\sigma_{rz}}{r}-\rho\frac{\partial^2u_z(r,\theta,t)}{\partial t^2}=0. \tag{3}$$

Stress components in the above equations can be substituted in terms of displacement components. Since displacement components are functions of wave forms, time dependency of waves must be established.

Wave Form

In cylindrical geometry the generation of surface waves in the circumferential direction with a plane wave front requires the circumferential wave speed to be a function of the radial distance. Viktorov [1] has introduced this concept and called it the angular wave number. Similar formulation has been adapted here:

$$u_r(r,\theta,t)=U_r(r)e^{i(p\theta-\omega t)}$$

$$u_\theta(r,\theta,t)=U_t(r)e^{i(p\theta-\omega t)}$$

$$u_z(r,\theta,t)=U_z(r)e^{i(p\theta-\omega t)} \tag{4}$$

where $U_r(r)$, $U_t(r)$, and $U_z(r)$ represent the amplitude of vibration in the radial, tangential, and axial directions, respectively. "i" is the imaginary number $\sqrt{-1}$. It should be noted here that the phase velocity is not a constant and changes with radius. As shown in Fig. 1 the phase velocity has to be proportional to the radius to have a plane wave front. Hence, if c_b is assumed to be the phase velocity at the outer surface with radius b; for other points having a radius r the phase velocity would be

$$v_{ph}(r)=c_br/b. \tag{4a}$$

For the flat-plate case wave number k is defined as ω/v_{ph} because curvature does not change. However, for a curved plate the same definition would be r dependent. Thus the angular wave number p, which is independent of r is defined as

$$p=\omega/(v_{ph}(r)/r)=\omega b/c_b. \tag{4b}$$

Governing Differential Equations

Subsequent substitution of Eqs. (4), (1), and (2) into Eq. (3) yields the following governing differential equations:

$$
\begin{aligned}
&-2C_{5,5}U_r(r)p^2-2C_{1,5}U_t(r)p^2-2C_{4,5}U_z(r)p^2-2iC_{1,1}U_t(r)p\\
&\quad-2iC_{5,5}U_t(r)p-2iC_{1,4}U_z(r)p+4irC_{3,5}U_r'(r)p\\
&\quad+2irC_{1,3}U_t'(r)p+2irC_{5,5}U_t'(r)p+2irC_{3,4}U_z'(r)p\\
&\quad+2irC_{5,6}U_z'(r)p+2r^2\rho\omega^2U_r(r)-2C_{1,1}U_r(r)\\
&\quad+2C_{1,5}U_t(r)+2rC_{3,3}U_r'(r)-2rC_{1,5}U_t'(r)-2rC_{1,6}U_z'(r)\\
&\quad+2rC_{3,6}U_z'(r)+2r^2C_{3,3}U_r''(r)2r^2C_{3,5}U_t''(r)\\
&\quad+2r^2C_{3,6}U_z''(r)=0\\
&-2C_{1,5}U_r(r)p^2-2C_{1,1}U_t(r)p^2-2C_{1,4}U_z(r)p^2+2iC_{1,1}U_r(r)p\\
&\quad+2iC_{5,5}U_r(r)p+2iC_{4,5}U_z(r)p+2irC_{1,3}U_r'(r)p\\
&\quad+2irC_{5,5}U_r'(r)p+4irC_{1,5}U_t'(r)p+2irC_{1,6}U_z'(r)p\\
&\quad+2irC_{4,5}U_z'(r)p+2C_{1,5}U_r(r)+2r^2\rho\omega^2U_t(r)\\
&\quad-2C_{5,5}U_t(r)+2rC_{1,5}U_r'(r)+4rC_{3,5}U_r'(r)+2rC_{5,5}U_t'\\
&\quad+4rC_{5,6}U_z'(r)+2r^2C_{3,5}U_r''(r)+2r^2C_{5,5}U_t''(r)\\
&\quad+2r^2C_{5,6}U_z''(r)=0\\
&-2C_{4,5}U_r(r)p^2-2C_{1,4}U_t(r)p^2-2C_{4,4}U_z(r)p^2+2iC_{1,4}U_r(r)p\\
&\quad-2iC_{4,5}U_t(r)p+2irC_{3,4}U_r'(r)p+2irC_{5,6}U_r'(r)p\\
&\quad+2irC_{1,6}U_t'(r)p+2irC_{4,5}U_t'(r)p+4irC_{4,6}U_z'(r)p\\
&\quad+2r^2\rho\omega^2U_z(r)+2rC_{1,6}U_r'(r)+2rC_{3,6}U_r'(r)\\
&\quad+2rC_{6,6}U_z'(r)+2r^2C_{3,6}U_r''(r)+2r^2C_{5,6}U_t''(r)\\
&\quad+2r^2C_{6,6}U_z''(r)=0. \qquad (5)
\end{aligned}
$$

Boundary Conditions

In order to obtain the dispersion curves, the traction-free boundary conditions (zero stress values on the inner and outer surfaces of the pipe) must be satisfied. Hence, at $r=a$ and $r=b$:

$$
\begin{aligned}
&C_{1,3}U_r(r)+ipC_{3,5}U_r(r)+ipC_{1,3}U_t(r)-C_{3,5}U_t(r)+ipC_{3,4}U_z(r)\\
&\quad+rC_{3,3}U_r'(r)+rC_{3,5}U_t'(r)+rC_{3,6}U_z'(r)=0\\
&C_{1,5}U_r(r)+ipC_{5,5}U_r(r)+ipC_{1,5}U_t(r)-C_{5,5}U_t(r)-ipC_{4,5}U_z(r)\\
&\quad+rC_{3,5}U_r'(r)+rC_{5,5}U_t'(r)+rC_{5,6}U_z'(r)=0\\
&C_{1,6}U_r(r)+ipC_{5,6}U_r(r)+ipC_{1,6}U_t(r)-C_{5,6}U_t(r)+ipC_{4,6}U_z(r)\\
&\quad+rC_{3,6}U_r'(r)+rC_{5,6}U_t'(r)+rC_{6,6}U_z'(r)=0. \qquad (6)
\end{aligned}
$$

Solution

It can be seen that all differential equations are functions of three displacement components and their derivatives. It should be also noted that $U_r(r)$, $U_t(r)$, and $U_z(r)$ are functions of the radius only and they appear in all equations. Therefore, there are three coupled differential equations and six boundary conditions that must be satisfied simultaneously.

To solve the equations, the unknown functions are expanded in Fourier series (FS). Substitution of FS expansions into the differential equations provides three algebraic equations that must be satisfied for the entire problem domain. To satisfy the equations for a given number of FS terms weighted residuals integration with a linear weight function has been utilized:

$$
R=\int_a^b wf(r,x_i)dr=0. \qquad (7)
$$

The radius corresponding to the peak value of the linear weight function can take any value between the inner and the outer radius, each resulting one independent equation. Hence from every differential equation any number of equations can be obtained.

On the other hand, it is known that the general solution is a linear combination of all solution functions that can be obtained. Therefore, the general solution should contain combinatorial parameters. The number of combinatorial parameters is the same as the number of individual solutions. These combinatorial parameters are necessary to satisfy the boundary conditions. Satisfaction of six boundary conditions requires six parameters and six equations. Therefore the necessary and sufficient number of combinatorial parameters is six and it indicates the existence of six independent solutions.

Substitution of solution functions into the differential equations leads to three equations, each containing all of the FS parameters. In other words, all FS parameters for the three amplitude functions appear in every equation. Because of this coupling, the values of parameters obtained for FS expansion of $U_r(r)$, $U_t(r)$, and $U_z(r)$ are not independent and a solution must yield all parameters as one set of results. Since the equations are linear and the results must be combined using combinatorial parameters only their relative values must be found. Therefore one of the FS parameters can be assumed equal to one. Then the relative values for other FS parameters can be calculated in terms of this unit value. Each set of the parameter values defines a set of dependent shapes for the above amplitude functions; these are called basic shapes. Since the number of equations must be equal to the number of unknowns a specific number of weight functions are required.

The FS expansion for $U_r(r)$ can be written as

$$
U_r(r)=x_0+\sum_{n=1}^{m}\left(\cos\left(\frac{n\pi r}{L}\right)x_n+\sin\left(\frac{n\pi r}{L}\right)y_n\right) \qquad (8)
$$

which contains $2m+1$ parameters or coefficients, x_n and y_n.

With two other expressions for $U_t(r)$ and $U_z(r)$ the number of unknowns increases to $6m+3$. Performing weighted residuals method, a set of linear equations results:

$$
\begin{pmatrix}
a_{1,1}x_1 & a_{1,2}x_2 & \cdots & a_{1,s}x_s & a_{1,s+1}x_{s+1} & \cdot & a_{1,s+6}x_{s+6}\\
a_{2,1}x_1 & a_{2,2}x_2 & \cdots & a_{2,s}x_s & a_{2,s+1}x_{s+1} & \cdot & a_{2,s+1}x_{s+6}\\
\cdot & \cdot & \cdots & \cdot & \cdot & \cdot & \cdot\\
\cdot & \cdot & \cdots & \cdot & \cdot & \cdot & \cdot\\
\cdot & \cdot & \cdots & \cdot & \cdot & \cdot & \cdot\\
a_{s,1}x_1 & a_{s,2}x_2 & \cdots & a_{s,s}x_s & a_{s,s+1}x_{s+1} & \cdot & a_{s,s+6}x_{s+6}
\end{pmatrix}
=\begin{pmatrix}0\\0\\\cdot\\\cdot\\\cdot\\0\end{pmatrix} \qquad (9)
$$

where $x_{s+1}, x_{s+2}, \ldots, x_{s+6}$ represent the last sine and cosine terms of FS expansions. Assigning six independent unit vectors to the last six parameters as shown in Eq. (10),

$$\begin{pmatrix} x^1_{s+1} & x^2_{s+1} & x^3_{s+1} & x^4_{s+1} & x^5_{s+1} & x^6_{s+1} \\ x^1_{s+2} & x^2_{s+2} & x^3_{s+2} & x^4_{s+2} & x^5_{s+2} & x^6_{s+2} \\ x^1_{s+3} & x^2_{s+3} & x^3_{s+3} & x^4_{s+3} & x^5_{s+3} & x^6_{s+3} \\ x^1_{s+4} & x^2_{s+4} & x^3_{s+4} & x^4_{s+4} & x^5_{s+4} & x^6_{s+4} \\ x^1_{s+5} & x^2_{s+5} & x^3_{s+5} & x^4_{s+5} & x^5_{s+5} & x^6_{s+5} \\ x^1_{s+6} & x^2_{s+6} & x^3_{s+6} & x^4_{s+6} & x^5_{s+6} & x^6_{s+6} \end{pmatrix} = \begin{pmatrix} 1 & 0 & 0 & 0 & 0 & 0 \\ 0 & 1 & 0 & 0 & 0 & 0 \\ 0 & 0 & 1 & 0 & 0 & 0 \\ 0 & 0 & 0 & 1 & 0 & 0 \\ 0 & 0 & 0 & 0 & 1 & 0 \\ 0 & 0 & 0 & 0 & 0 & 1 \end{pmatrix} \tag{10}$$

yields six independent solutions. Therefore the number of equations has to be $s=6m-3$. Consequently, the general solution can be obtained as a linear combination of the above solutions:

$$A_1 \begin{pmatrix} 1_1 \\ x^1_2 \\ \cdot \\ \cdot \\ \cdot \\ x^1_s \end{pmatrix} + A_2 \begin{pmatrix} x^2_1 \\ x^2_2 \\ \cdot \\ \cdot \\ \cdot \\ x^2_s \end{pmatrix} + A_3 \begin{pmatrix} x^3_1 \\ x^3_2 \\ \cdot \\ \cdot \\ \cdot \\ x^3_s \end{pmatrix} + A_4 \begin{pmatrix} x^4_1 \\ x^4_2 \\ \cdot \\ \cdot \\ \cdot \\ x^4_s \end{pmatrix} + A_5 \begin{pmatrix} x^5_1 \\ x^5_2 \\ \cdot \\ \cdot \\ \cdot \\ x^5_s \end{pmatrix} + A_6 \begin{pmatrix} x^6_1 \\ x^6_2 \\ \cdot \\ \cdot \\ \cdot \\ x^6_s \end{pmatrix} . \tag{11}$$

The superscript for FS parameters shows the solution set number. Substitution of the obtained FS parameters into stress components on the inner and outer surfaces of the pipe leads to an eigenvalue problem. The determinant of the coefficients of A_i should be zero for any point located on the dispersion curves.

Numerical Results

Based on the proposed mathematical modeling a Mathematica program has been developed. To ensure the validity of the modeling and the computer program, its results are compared with the available dispersion curves for anisotropic flat plates by using small ratios of thickness to radius, when pipe geometry approaches flat plate geometry. Additionally, the results are compared with the published results for isotropic pipes ([2]). Since the exact input values have not been reported by Qu et al. [2], the comparison is done only qualitatively. The dispersion curves are also given for anisotropic pipes.

A Comparison With Available Data for Isotropic Flat Plate. Dispersion curves for a flat plate are given in Mal and Singh [11], see Fig. 3. Curves for the same plate thickness and material properties, but having an outer radius of 1 m, are generated by the proposed method and shown in Fig. 4.

A comparison of Figs. 3 and 4 shows a very good match between the two when only 20 terms are used in the FS expansions.

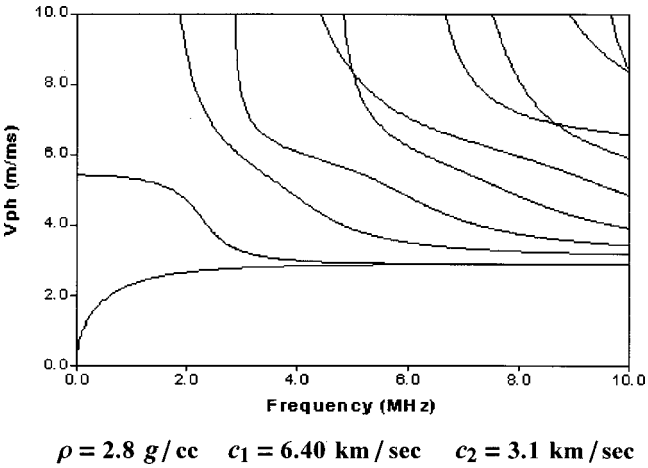

Fig. 3 Dispersion curves for isotropic flat plate ([11]). Plate thickness=1 mm.

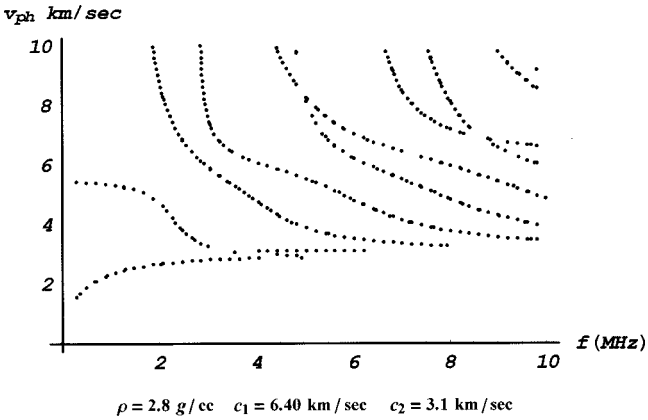

Fig. 4 Dispersion curves generated by the proposed method. Plate thickness=1 mm. Pipe outside radius=1.0 m.

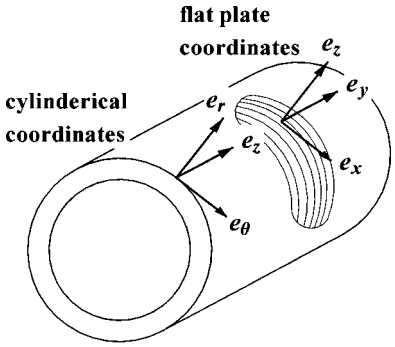

Fig. 5 Tangential direction of the fibers maintains the symmetry. Coordinate systems for flat-plate and pipe analyses are also shown.

B Comparison With Available Data for Anisotropic Flat Plate. Dispersion curves for anisotropic flat plates are available in the literature ([12,13]). In this section our results are compared with those given in Rose [13].

For the unidirectional composite plate or pipe with a zero-degree angle between the wave propagation direction and the fiber direction as shown in Fig. 5, the material and the geometric symmetry conditions are maintained; hence, the plain-strain formulation remains valid. Consequently the constitutive matrix reduces to the following form:

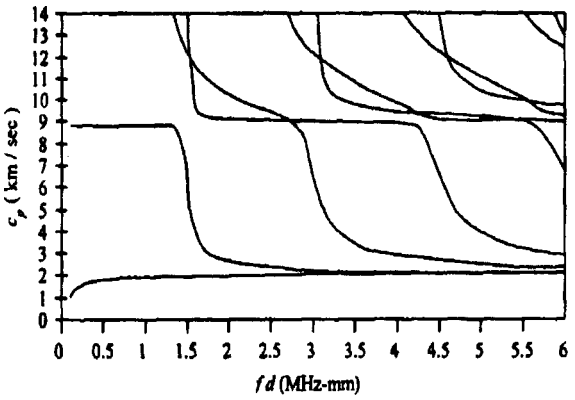

Fig. 6 Dispersion curves of a unidirectional composite plate for waves propagating in fiber direction (*x*-axis direction, 0 deg). Material properties are given in Eq. (12), $\rho = 1580$ kg/m^3 ([3]).

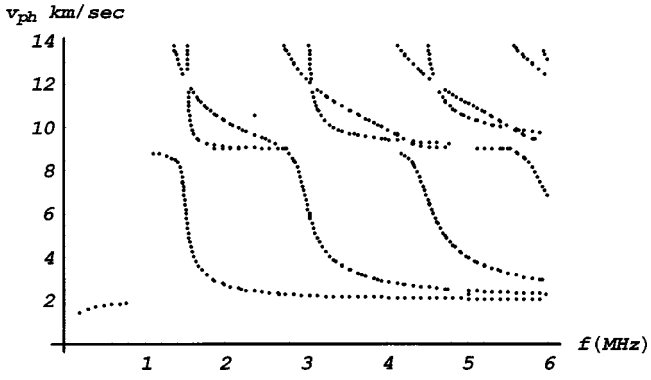

Fig. 7 Dispersion curves for a large-diameter pipe made of an anisotropic material. Material properties are given in Eq. (12). Pipe wall thickness = 1 mm. Pipe outer radius = 1000 mm, $m = 30$.

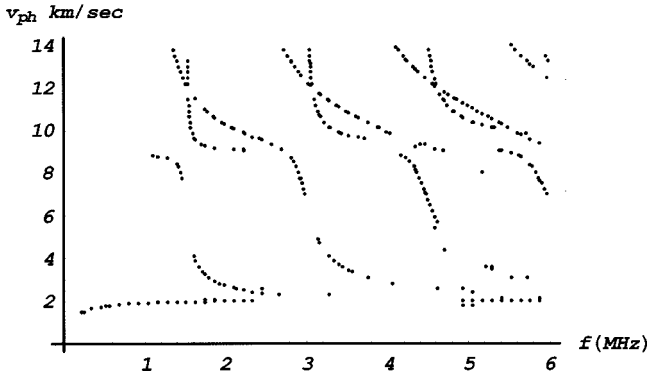

Fig. 8 Dispersion curves for the anisotropic pipe with $m = 20$. Pipe dimensions and material properties are same as in Fig. 7, only *m* is different.

$$\begin{pmatrix} \sigma_{\theta\theta} \\ \sigma_{zz} \\ \sigma_{rr} \\ \sigma_{r\theta} \end{pmatrix} = \begin{pmatrix} 128.2 & 6.9 & 6.9 & 0 \\ 6.9 & 14.95 & 7.33 & 0 \\ 6.9 & 7.33 & 14.95 & 0 \\ 0 & 0 & 0 & 6.73 \end{pmatrix} \begin{pmatrix} e_{\theta\theta} \\ 0 \\ e_{rr} \\ 2e_{r\theta} \end{pmatrix}. \quad (12)$$

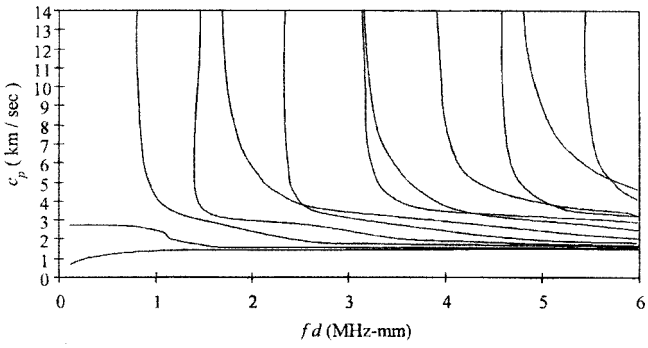

Fig. 9 Dispersion curves of unidirectional composite plate for waves propagating perpendicular to the fiber direction (*x*-axis direction, 90 deg). Material properties are given in Eq. (13). Plate thickness = 1 mm, $\rho = 1580$ kg/m^3 ([3]).

Stiffness values are given in GPa. Flat-plate results are shown in Fig. 6. Results for the curved plate are shown in Figs. 7 and 8.

The result of Fig. 7 is obtained using 30 terms ($m = 30$) in the Fourier series expansion. To show the effect of the number of terms (m) on the computed results the same dispersion curves are computed for $m = 20$ and shown in Fig. 8.

It is interesting to note that smaller value of m gives broken lines. Therefore the user can easily realize the need for a greater number of terms in the FS expansion when the lines in the dispersion curve plot are found broken. There are some missing parts of curves in Fig. 7 that can be obtained by increasing m. However, for $m = 30$ we get enough information for comparison with the results given by Rose [13].

For the same material with fibers going in the longitudinal direction of the pipe, the constitutive matrix changes to Eq. (13).

$$\begin{pmatrix} \sigma_{\theta\theta} \\ \sigma_{zz} \\ \sigma_{rr} \\ \sigma_{r\theta} \end{pmatrix} = \begin{pmatrix} 14.95 & 6.9 & 7.33 & 0 \\ 6.9 & 128.2 & 6.9 & 0 \\ 7.33 & 6.9 & 14.95 & 0 \\ 0 & 0 & 0 & 3.81 \end{pmatrix} \begin{pmatrix} e_{\theta\theta} \\ 0 \\ e_{rr} \\ 2e_{r\theta} \end{pmatrix}. \quad (13)$$

Obtained results for this case also match with the corresponding dispersion curves presented by Rose [13]; see Figs. 9 and 10.

For the case where fibers are oriented at 45 deg relative to the pipe axis, plane-strain assumptions are no longer valid. The constitutive matrix for this case is obtained by transformation of the coordinate system as shown in Eq. (14). See Figs. 11(*a*), 11(*b*) and 12 for comparison. This case also shows an excellent match between the available data and the obtained results.

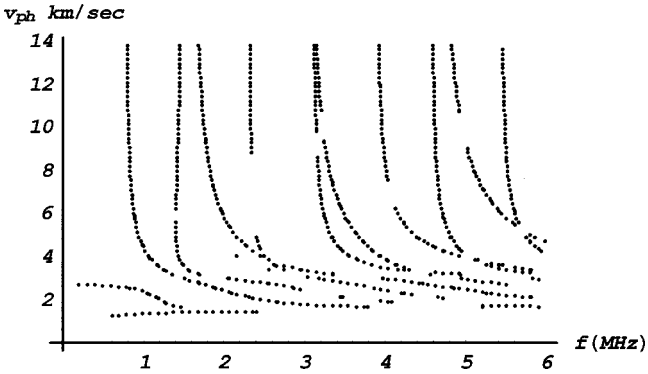

Fig. 10 Computed dispersion curves for an anisotropic large diameter pipe, when fiber and wave propagation directions are perpendicular to each other. Material properties are given in Eq. (13). Pipe wall thickness = 1 mm. Pipe outer radius = 1000 mm.

$$\begin{pmatrix}\sigma_{\theta,\theta}\\ \sigma_{z,z}\\ \sigma_{r,r}\\ \sigma_{z,r}\\ \sigma_{\theta,r}\\ \sigma_{\theta,z}\end{pmatrix}=\begin{pmatrix}45.9675 & 32.5075 & 7.115 & 0 & 0 & -28.3125\\ 32.5075 & 45.9675 & 7.115 & 0 & 0 & -28.3125\\ 7.115 & 7.115 & 14.95 & 0 & 0 & 0.215\\ 0 & 0 & 0 & 5.27 & -1.46 & 0\\ 0 & 0 & 0 & -1.46 & 5.27 & 0\\ -28.3125 & -28.3125 & 0.215 & 0 & 0 & 32.3375\end{pmatrix}\begin{pmatrix}e_{\theta,\theta}\\ e_{z,z}\\ e_{r,r}\\ 2e_{z,r}\\ 2e_{\theta,r}\\ 2e_{\theta,z}\end{pmatrix} \tag{14}$$

Since for the curved plate, the midplane is not the plane of symmetry, the dispersion curves cannot be grouped as symmetric and antisymmetric modes. That is why all modes are shown together in Fig. 12 for a large-diameter pipe.

C Comparison With Available Data for Isotropic Pipe As mentioned earlier, Qu et al. [2] have derived dispersion curves for aluminum pipes but the material properties have not been reported in their work. Hence, the quantitative comparison was not possible. However, curves presented here, Fig. 13, qualitatively look similar to those of Qu et al. [2], Fig. 14. Figures 13 and 14 show the obtained dispersion curves with non-dimensional $\bar{k}$ and $\bar{\omega}$ where $\bar{k}=k(b-a)$ and

$$\bar{\omega}=\omega(b-a)\sqrt{\frac{\rho}{\mu}}.$$

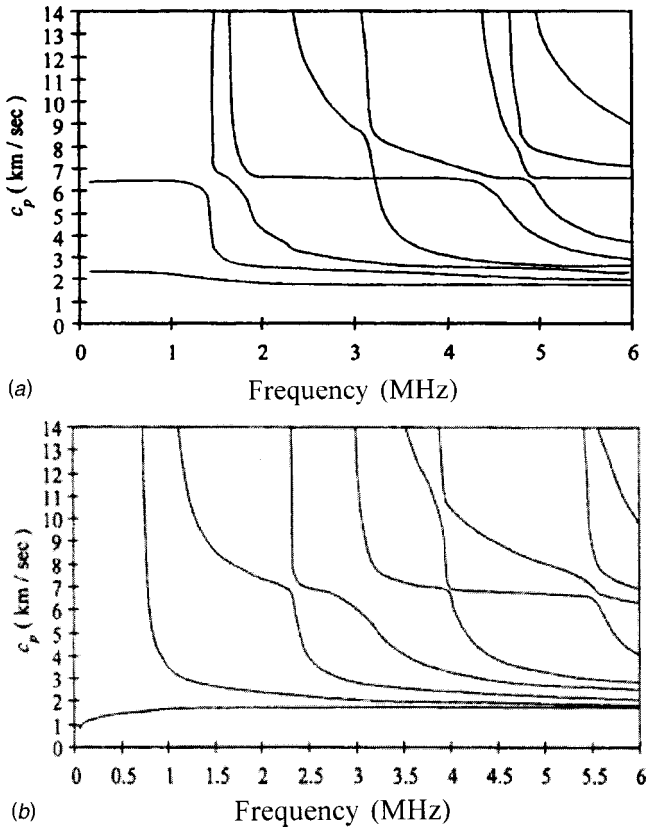

Fig. 11 (*a*) Dispersion curves for symmetric modes for a unidirectional composite plate for waves propagating in 45 deg to the fiber direction. Plate thickness=1 mm and ρ=1580 kg/m^3 ([3]). (*b*) Dispersion curves for antisymmetric modes for a unidirectional composite plate for waves propagating in 45 deg to the fiber direction. Plate thickness=1 mm and ρ=1580 kg/m^3 ([3]).

D Anisotropic Pipe of Small Radius of Curvature. To show the effect of the radius of curvature on the dispersion curves the pipe radius is varied from 1000 mm to 2.5 mm keeping the wall thickness and material properties same as those mentioned in the figure captions for Figs. 7 and 9. Dispersion curves obtained by the 30 terms FS expansion for $r=1000$, 10, 5, and 2.5 mm are shown in Figs. 15 and 16. Figure 15 shows dispersion curves for fibers going in the circumferential direction and Fig. 16 is for fibers going in the axial direction while the waves propagate in the circumferential directions in both cases.

From Figure 15 one can see that for fibers oriented in the circumferential direction the dispersion curves do not change significantly as the outer radius (r) is reduced from 1000 mm to 10 mm. However, as r is reduced further the deviation of the dispersion curves from the large radius case is no longer negligible. For

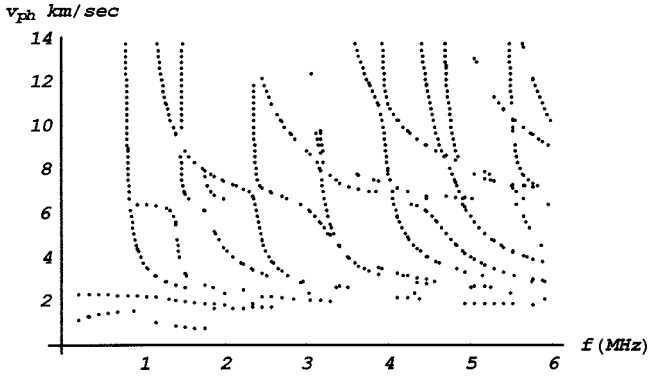

Fig. 12 Dispersion curves for a large diameter pipe made of an anisotropic material. Material properties are given in Eq. (14). Pipe wall thickness=1 mm. Pipe outer radius=1000 mm, m =25.

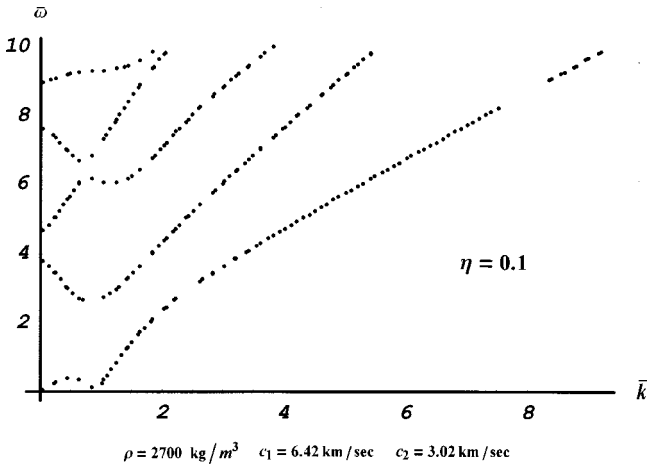

Fig. 13 Dispersion curves for aluminum pipe obtained by the proposed method. η (ratio of inner to outer radius)=0.1.

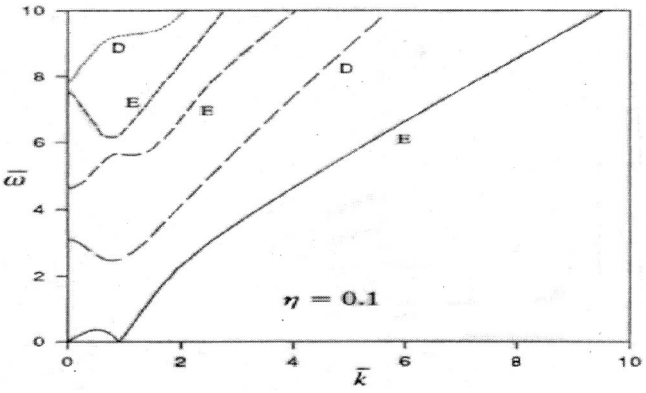

Fig. 14 Dispersion curves for aluminum pipe obtained by Qu et al. [2]. Material properties are not known.

fibers oriented in the axial direction (Fig. 16) the dispersion curves remain almost unchanged for $r = 1000$ mm down to 2.5 mm. For $r = 2.5$ mm the dispersion curves are obtained with $m = 45$ in FS expansion of amplitude functions. The computation with $m = 30$ gave too many broken lines in the dispersion curve plot for $r = 2.5$ mm.

In summary, a comparison between Figs. 15 and 16 shows that the effect of curvature is stronger when the fibers are oriented along the circumferential direction and hence when the fibers also have a curvature. When the fibers are oriented in the axial direction and hence don't have any curvature the flat-plate approximation can be extended to pipes of much lower radius.

Dispersion curves for the 5-mm outer radius pipe with fibers oriented along the 45 deg direction are shown in Fig. 17. This result is obtained for the material properties given in Eq. (14). In the frequency range smaller than 1 MHz, some vertical lines appeared due to the numerical errors when the number (m) of FS terms is 25. By increasing m to 35 those lines disappeared. The results for $m = 35$ are shown on the left side of Fig. 17.

Conclusion

A solution technique based on the Fourier series expansion of the unknown quantities has been introduced to solve the elastic wave propagation problem in anisotropic cylindrical plates in the circumferential direction. Accuracy of the technique has been verified by comparing the computed results for isotropic pipes with the published results. Since no published results are available for wave propagation in the circumferential direction in anisotropic cylindrical plates, the computed dispersion curves for anisotropic curved plates could not be compared with any results available in the literature. However, the Lamb wave dispersion curves for flat plates can be computed and those values are used to check the accuracy of the proposed technique. With the new technique, dispersion curves for cylindrical plates with large radius of curvature (outer radius of curvature to thickness ratio equal to 1000) have been computed and compared with the flat-plate results for both isotropic and anisotropic materials. Computed results for such low curvature plates matched very well with the flat-plate results. The effect on the dispersion curves as the curvature of the anisotropic plate increases has been also studied.

The solution technique used for this specific wave propagation

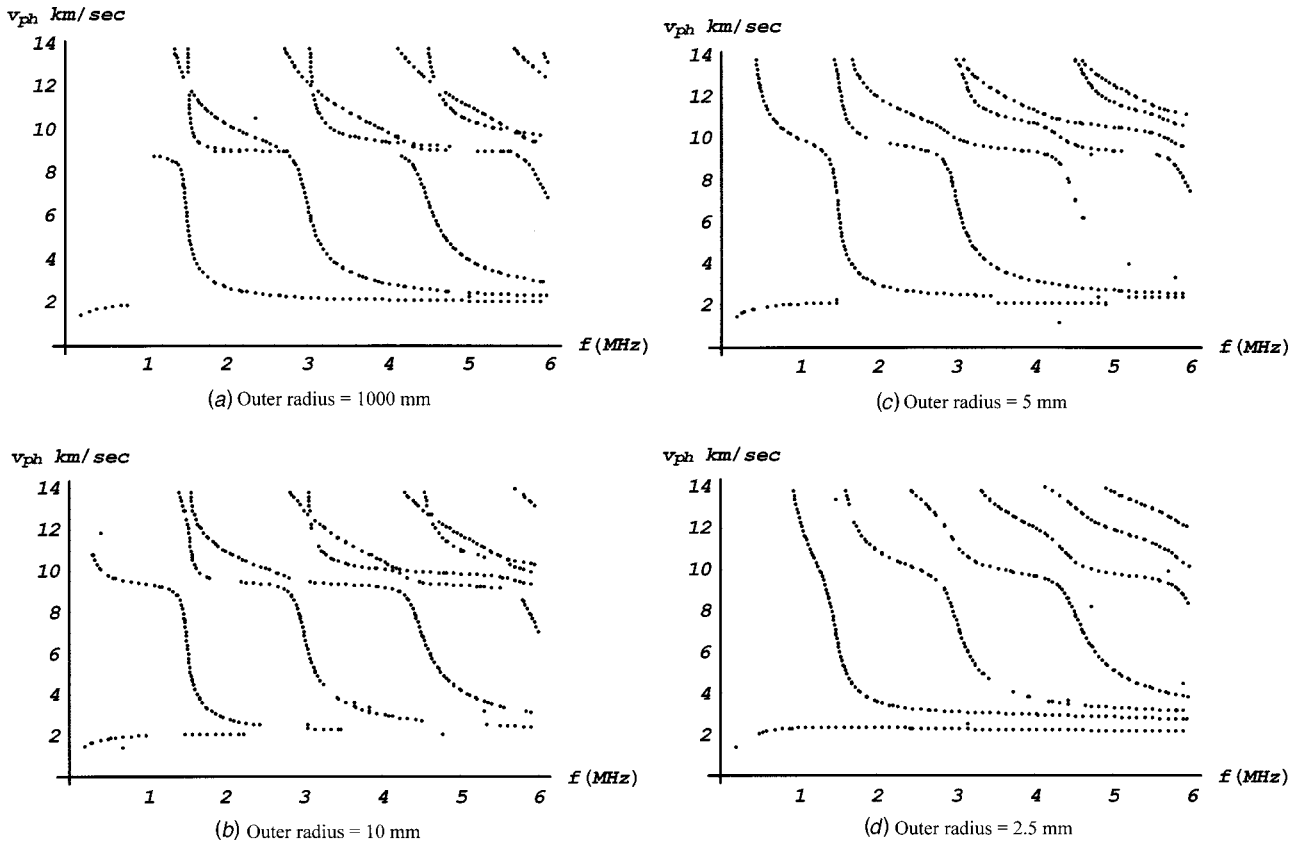

Fig. 15 Dispersion curves for circumferential direction wave propagation in fiber-reinforced cylindrical composite plates when fibers are oriented in the circumferential direction, outer radius of the pipe is (*a*) 1000 mm, (*b*) 10 mm, (*c*) 5 mm, and (*d*) 2.5 mm. Pipe wall thickness and material properties are same as those in Fig. 7.

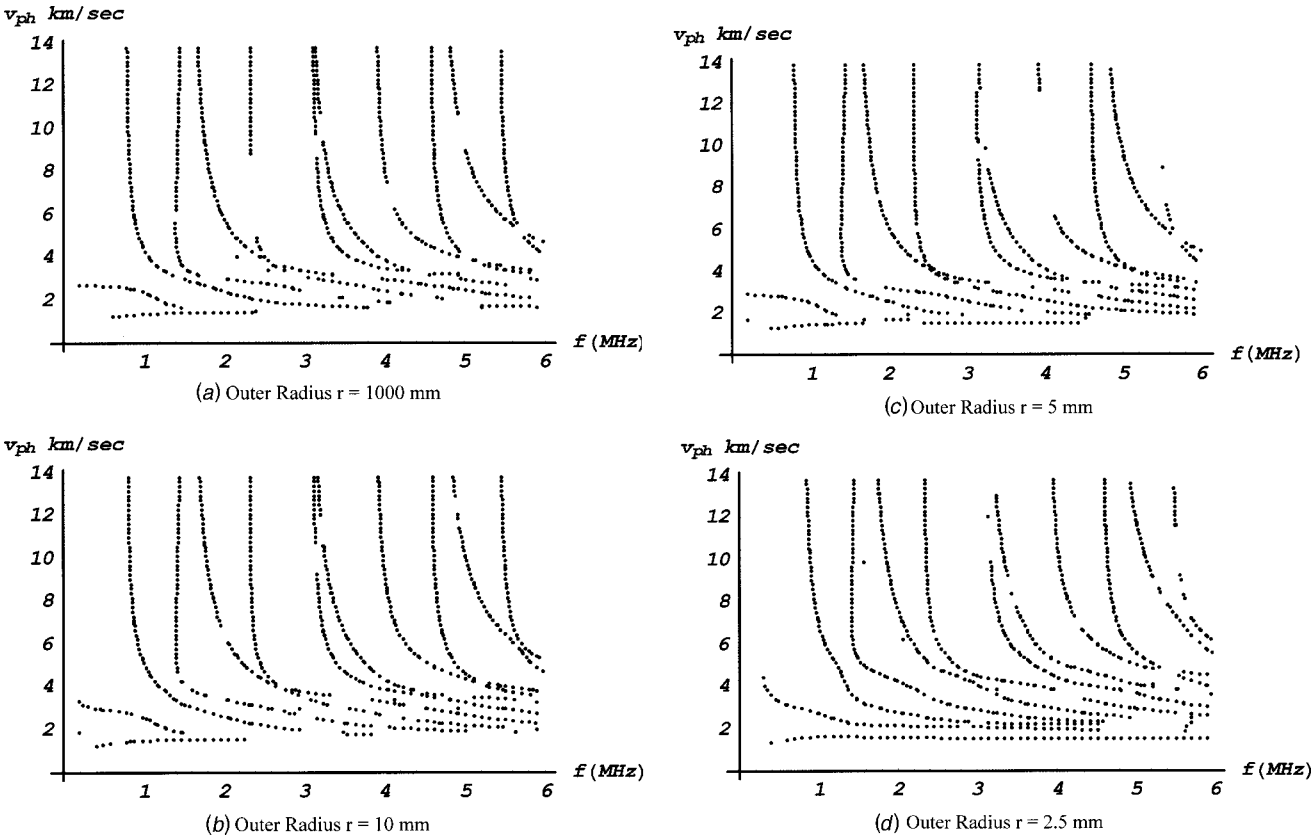

Fig. 16 Dispersion curves for circumferential direction wave propagation in fiber-reinforced composite cylindrical plates when fibers are oriented in the axial direction, outer radius of the pipe is (*a*) 1000 mm, (*b*) 10 mm, (*c*) 5 mm, and (*d*) 2.5 mm. Pipe wall thickness and material properties are same as those in Fig. 9.

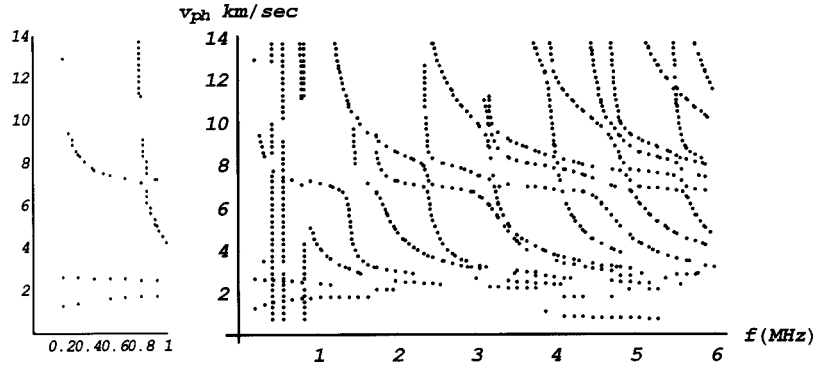

Fig. 17 Dispersion curves for the curved plate when the fibers are oriented in the 45 deg direction. Material properties are given in Eq. (14). Outer radius is 5 mm. Thickness=1 mm. Right figure is for $m=25$, and the left figure is for $m=35$. Frequency range for the left figure is 0 to 1 MHz and for the right figure it is 0 to 6 MHz.

problem is a newly developed general solution technique for solving a coupled partial differential equation set ([14]). Applicability of this technique to other wave propagation problems is currently under investigation.

Acknowledgment

This research was partially supported from the National Science Foundation grant CMS-9901221.

References

[1] Viktorov, I. A., 1958, ''Rayleigh-Type Waves on a Cylindrical Surface,'' Sov. Phys. Acoust., **4**, pp. 131–136.

[2] Qu. J., Berthelot, Y., and Li, Z., 1996, ''Dispersion of Guided Circumferential Waves in a Circular Annulus,'' *Review of Progress in Quantitative Nondestructive Evaluation*, D. O. Thompson and D. E. Chimenti, eds., Plenum, New York, **15**, pp. 169–176.

[3] Grace, O. D., and Goodman, R. R., 1966, ''Circumferential Waves on Solid Cyliners,'' J. Acoust. Soc. Am., **39**, pp. 173–174.

[4] Brekhovskikh, L. M., 1968, ''Surface Waves Confined to the Curvature of the Boundary in Solid,'' Sov. Phys. Acoust., **13**, pp. 462–472.

[5] Cerv, J., 1988, ''Dispersion of Elastic Waves and Rayleigh-Type Waves in a Thin Disc,'' Acta Tech. CSAV, **89**, pp. 89–99.
[6] Liu, G., and Qu, J., 1998, ''Guided Circumferential Waves in a Circular Annulus,'' ASME J. Appl. Mech., **65**, pp. 424–430.
[7] Liu, G., and Qu, J., 1998, ''Transient Wave Propagation in a Circular Annulus Subjected to Impulse Excitation on Its Outer Surface,'' J. Acoust. Soc. Am., **103**, pp. 1210–1220.
[8] Valle, C., Qu, J., and Jacobs, L. J., 1999, ''Guided Circumferential Waves in Layered Cylinders,'' Int. J. Eng. Sci., **37**, pp. 1369–1387.
[9] Nayfeh, A. H., 1995, *Wave Propagation in Layered Anisotropic Media With Application to Composites*, Elsevier, Amsterdam.
[10] Armenakas, A. E., and Reitz, E. S., 1973, ''Propagation of Harmonic Waves in Orthotropic, Circular Cylindrical Shell,'' ASME J. Appl. Mech., **40**, pp. 168–174.
[11] Mal, A. K., and Singh, S. J., 1991, *Deformation of Elastic Solids*, Prentice-Hall, Englewood Cliffs, NJ, p. 313.
[12] Karim, M. R., Mal, A. K., and Bar-Cohen, Y., 1990, ''Inversion of Leaky Lamb Wave Data by Simplex Algorithm,'' J. Acoust. Soc. Am., **88**, pp. 482–491.
[13] Rose, J. L., 1999, *Ultrasonic Waves in Solid Media*, Cambridge University Press, Cambridge, U.K., pp. 264–271.
[14] Towfighi, S., 2001, ''Elastic Wave Propagation in Circumferential Direction in Anisotropic Pipes,'' Ph.D. dissertation, The University of Arizona, Tucson, AZ.